

ОСОБЕННОСТИ СОСТАВА ПЛАЗМЫ И КИНЕТИКИ АТОМОВ ФТОРА В СМЕСИ $\text{CHF}_3 + \text{O}_2$ **А.М. Ефремов, Д.Е. Башмакова, К.-Н. Kwon**

Александр Михайлович Ефремов (ORCID 0000-0002-9125-0763)*, Дарья Евгеньевна Башмакова
Ивановский государственный химико-технологический университет, Шереметевский просп., 7, Иваново,
Российская Федерация, 153000
E-mail: amefremov@mail.ru*

Kwang-Ho Kwon (ORCID 0000-0003-2580-8842)
Korea University, 208 Seochang-Dong, Chochiwon, Korea, 339-800
E-mail: kwonkh@korea.ac.kr

Исследовано влияние начального состава смеси $\text{CHF}_3 + \text{O}_2$ на электрофизические параметры плазмы, стационарные концентрации активных частиц и кинетику атомов фтора в условиях постоянства давления газа и вкладываемой мощности. При совместном использовании диагностики плазмы зондами Ленгмюра и модельного анализа кинетики плазмохимических процессов подтверждены известные из предшествующих работ особенности состава плазмы в отсутствие кислорода (в частности – доминирование молекул HF в газовой фазе). Выявлены механизмы влияния кислорода на стационарные концентрации нейтральных частиц через кинетику процессов при электронном ударе и кинетику атомно-молекулярных реакций. Установлено, что увеличение доли кислорода в смеси при пропорциональном снижении содержания CHF_3 : а) приводит к заметным изменениям параметров электронной и ионной компонент плазмы (средней энергии и концентрации электронов, плотности потока ионов); б) обеспечивает эффективную конверсию фторуглеродных радикалов CHF_x и CF_x в соединения вида CF_xO , FO и CO_x ; в) сопровождается ростом концентрации атомов фтора вплоть до 50% O_2 в смеси. Последний эффект противоречит изменению суммарной скорости генерации атомов, но обусловлен снижением частоты их гибели в газофазных реакциях семейства $\text{CHF}_x + \text{F} \rightarrow \text{CF}_x + \text{HF}$. Проведен модельный анализ кинетики гетерогенных процессов с использованием отслеживающих параметров, основанных на характеристиках газовой фазы. Показано, что добавка кислорода способствует снижению полимеризационной способности плазмы из-за уменьшения плотности потока полимеробразующих частиц и роста скорости окислительной деструкции осаждаемой полимерной пленки.

Ключевые слова: CHF_3 , O_2 , плазма, параметры, активные частицы, ионизация, диссоциация, травление, полимеризация

**FEATURES OF PLASMA COMPOSITION AND FLUORINE ATOM KINETICS
IN $\text{CHF}_3 + \text{O}_2$ GAS MIXTURE****A.M. Efremov, D.E. Bashmakova, K.-H. Kwon**

Alexander M. Efremov (ORCID 0000-0002-9125-0763)*, Daria E. Bashmakova
Ivanovo State University of Chemistry and Technology, Sheremetevskiy ave., 7, Ivanovo, 153000, Russia
E-mail: amefremov@mail.ru*

Kwang-Ho Kwon (ORCID 0000-0003-2580-8842)
Korea University, 208 Seochang-Dong, Chochiwon, Korea, 339-800
E-mail: kwonkh@korea.ac.kr

The effects of initial composition of $\text{CHF}_3 + \text{O}_2$ gas mixture on electro-physical plasma parameters, steady-state densities of active species and fluorine atom kinetics were investigated

under the condition of constant gas pressure and input power. The combination of plasma diagnostics by Langmuir probes and model-based analysis of plasma chemistry confirmed known from previous work features of plasma composition in the absence of oxygen (in particular, the domination of HF molecules in a gas phase) as well as demonstrated how the oxygen influences steady-state densities of neutral species through kinetics of both electron-impact and atom-molecular reactions. It was shown that the addition of O₂ with a proportional decrease in the content of CHF₃ a) results in noticeable changes in electrons- and ions-related plasma parameters (electron temperature, electron density, ion flux); b) provides the effective conversion of fluorocarbon radicals (CHF_x, CF_x) into such compounds as CF_xO, FO and CO_x; and b) causes an increase in the fluorine atom density up to 50% O₂. The last phenomenon contradicts with the change in the total F atom formation rate, but reflects a decrease of their loss frequency in the reaction family of CHF_x + F → CF_x + HF. The model-based analysis of heterogeneous process kinetics was carried out using the set of tracing parameters based on gas-phase plasma characteristics. It was found that the addition of oxygen lowers the plasma polymerizing ability through both decreasing flux of polymerizing species and accelerating the oxidative destruction of deposited polymer film.

Key words: CHF₃, O₂, plasma, parameters, active species, ionization, dissociation, etching, polymerization

Для цитирования:

Ефремов А.М., Башмакова Д.Е., Кwon К.-Н. Особенности состава плазмы и кинетики атомов фтора в смеси CHF₃ + O₂. *Изв. вузов. Химия и хим. технология*. 2023. Т. 66. Вып. 1. С. 48–55. DOI: 10.6060/ivkkt.20236601.6667.

For citation:

Efremov A.M., Bashmakova D.E., Kwon K.-H. Features of plasma composition and fluorine atom kinetics in CHF₃ + O₂ gas mixture. *ChemChemTech [Изв. Vyssh. Uchebn. Zaved. Khim. Khim. Tekhnol.]*. 2023. V. 66. N 1. P. 48–55. DOI: 10.6060/ivkkt.20236601.6667.

INTRODUCTION

Fluorocarbon gases with a general formula of C_xH_yF_z have found numerous applications in the electronic device production industry for reactive-ion etching (RIE) of silicon and silicon-based compounds [1-3]. Being integrated into the standard photolithography cycle, RIE processes determine the surface patterning features and thus, influence the overall device quality and performance [1, 2]. Therefore, the development and optimization of RIE technologies are key tasks for obtaining devices with advanced characteristics.

From many published works [4-6], it can be understood that output RIE characteristics (etching rate, etching anisotropy and selectivity in respect to over- or under-layer material) strongly depend on the nature of fluorocarbon gas, and the principal feature is the z/x ratio in the original fluorocarbon molecule. For instance, the plasma excited in CF₄ (z/x = 4) exhibits high etching rates and good surface clearness, but simultaneously produces the nearly isotropic etching profile for Si and low SiO₂/Si etching selectivity [6, 7]. The reason is the combination of high density of F atoms with low density of less saturated fluorocarbon radicals that leads to the low polymerizing ability. On the contrary, the CHF₃ plasma (z/x = 3) provides the opposite situation in respect to densities of F and CF_x species [6, 8]. As a result, relatively low etching rates are accompanied by both anisotropic etching profile

(due to the protection of side walls by the fluorocarbon polymer film) [7] and high SiO₂/Si etching selectivity (due to the thinner polymer film on the oxygen-containing surface that leads to the better access for F atoms compared with Si) [7, 8]. It was found also that the effective tool to adjust the etching/polymerization balance is to combine the fluorocarbon gas with additive component which enforces or suppresses the polymerization. In particular, the addition of H₂ increases the polymer deposition rate due to the formation of CH_x radicals with higher sticking coefficients [9]. At the same time, the addition of O₂ lowers the density of CF_x radicals through CF_x + O/O(¹D) → CF_{x-1}O + F reaction family as well as causes the oxidative destruction of deposited polymer film [10, 11].

Though mixtures of fluorocarbons with various additive gases have been intensively studied during the last decade, the main attention was attracted to CF₄- and C₄F₈-based plasmas (see, for example, Refs. [11-15] and other ones cited in this works). As for CHF₃, there are only few works dealt with either oxygen-less CHF₃ + Ar plasmas [16, 17] or CHF₃ + O₂ + Ar [17, 18] plasmas with variable O₂/Ar mixing ratio at constant 50% of CHF₃. Obviously, the last case reflects chemical reaction kinetics and densities of plasma active species in the excess of CHF₃ and thus, does not cover all possible oxygen-related mixing effects. At the same time, Ref. [11] clearly demonstrated that CF₄/O₂ and O₂/Ar mixing ratios in the CF₄ + O₂ + Ar plasma produce

quite different changes in both steady-state plasma parameters and heterogeneous process kinetics.

The main idea of given work was to study the conventional binary $\text{CHF}_3 + \text{O}_2$ gas mixture where an increase in the fraction of additive gas appears through the substitution for CHF_3 . Accordingly, an increase in O_2 fraction in a feed gas by more than 50% provides the transition between O_2 -deficient and O_2 -excess reaction regimes. The main goals were 1) to compare how the change in CHF_3/O_2 mixing ratio does influence electrons- and ions related plasma parameters; 2) to analyze differences in densities of fluorine atoms and polymerizing radicals in the presence of oxygen; 3) to suggest features of etching and polymerization kinetics based on gas-phase plasma characteristics.

EXPERIMENTAL AND MODELING DETAILS

Experimental setup and procedures

Experiments were carried out in the inductively coupled plasma (ICP) reactor, the same as that used in our previous studies [11, 12]. Plasma was excited using the 13.56 MHz power supply connected to the planar copper coil at the top-side of the cylindrical reactor chamber. Another 13.56 MHz rf generator powered the bottom electrode in order to adjust the negative dc bias voltage ($-U_{dc}$) determining the ion bombardment energy (ε_i). Constant processing parameters were gas pressure ($p = 6$ mTorr), input power ($W_{inp} = 700$ W) and bias power ($W_{dc} = 200$ W). The latter corresponded to the non-constant $-U_{dc}$ which was changed oppositely to the behavior of ion flux. The variable parameter was the CHF_3/O_2 mixing ratio in a feed gas. In practice, various feed gas compositions were set by adjusting partial flow rates for CHF_3 and O_2 gases within the constant total gas flow rate (q) of 40 sccm. Accordingly, an increase of $q(\text{O}_2)$ in the range of 0-30 sccm caused the growth of the corresponding gas fraction $y(\text{O}_2) = q/q(\text{O}_2)$ from 0-75%. Simultaneously, the proportional decrease in $y(\text{CHF}_3)$ took place.

Plasma diagnostics was represented by the double Langmuir probe tool (DLP2000, Plasmart Inc.). The probe was installed through the viewport on the chamber side wall and was centered in the radial position. In order to minimize experimental errors due to the deposition of fluorocarbon polymer on probe tips, these were cleaned in 50% Ar + 50% O_2 plasma before and after each measurement. Our previous works [11-13] have demonstrated the efficiency of such procedure to provide correct plasma diagnostics data in high polymerizing fluorocarbon gases. The treatment of measured current-voltage (I-V) curves according to well-known statements of Langmuir probe theory for low pressure plasmas [4, 19] provided the data on electron

temperature (T_e) and ion current density (J_+). The latter also yielded the total density of positive ions (n_+).

Plasma modeling

In order to obtain the data on kinetics and densities of plasma active species, we applied a simplified 0-dimensional (global) plasma model. The kinetic scheme (the set of chemical reaction with corresponding rate coefficients) was taken from published works dealt with the modeling of $\text{CHF}_3 + \text{Ar}$ [16, 20] and $\text{CHF}_3 + \text{Ar} + \text{O}_2$ [18-21] and $\text{Ar} + \text{O}_2$ [22] plasmas. Comprehensive information on model assumptions and algorithm may be found in our previous works [16-20]. In particular, we accounted for typical features of low-pressure ($p < 20$ mTorr) and high-density ($n_+ > 10^{10}$ cm^{-3}) plasmas, such as:

- The electron energy distribution function (EEDF) is close to the Maxwellian one due to the essential contribution of equilibrium energy exchanges in electron-electron collisions [4]. Accordingly, rate coefficients for electron-impact processes may be obtained using fitting expressions $k = f(T_e)$ [10, 22, 23] resulted from the integration of Maxwellian EEDF with known process cross-sections.

- The electronegativity of both CHF_3 [16, 20] and O_2 [23] plasmas at $p < 20$ mTorr is low enough to suggest $n_+ \approx n_e$, where n_e is the electron density. Such situation is due to both high ionization degrees for neutral species ($n_+/N > 10^{-4}$, where $N = p/k_B T_g$ is the total gas density at the gas temperature of T_g) and low efficiency of dissociative attachment reactions. Accordingly, the dissociative attachment may also be excluded from the neutral species balance.

- The gas temperature is not sensitive to the gas mixing ratio and may be characterized by the constant value of ~ 600 K. The latter, in fact, represents the typical value for close processing conditions, reactor type and geometry [16-19].

- The loss of atoms and radicals on chamber walls follow the first-order recombination kinetics with nearly constant recombination probabilities [14, 22, 23]. In our case, the last suggestion was due to a) no re-deposition of any reaction products, except the steady-state fluorocarbon film; and b) the nearly constant internal wall temperature, as follows from the same feature for the extremal wall.

As model inputs, we used experimental data on T_e and J_+ . The output parameters were rates of plasma chemical reactions, volume-averaged steady-state densities of plasma active species and their fluxes to the etched surface.

Tracing parameters for heterogeneous kinetics

The basic features of heterogeneous processes in fluorocarbon-based plasmas have been discussed in

detail in published works [6-8, 11-13, 15-18, 24]. When summarizing their conclusions, one can suggest several gas-phase-related parameters to trace the influence of processing condition on both etching and polymerization kinetics. These are as follows:

- The rate of any ion-driven process has the rate of $Y_S \Gamma_+$, where Y_S is the ion-type-averaged process yield, and $\Gamma_+ \approx J_+/e$ is the ion flux. When taking in mind that the process yield is proportional to the momentum transferred from the incident ion to the surface atom [24, 25], one can assume $Y_S \sim (M_i \varepsilon_i)^{1/2}$ as well as trace the relative change in corresponding process kinetics by the parameter $G1 = (M_i \varepsilon_i)^{1/2} \Gamma_+$.

- The growth of polymer film is provided by $CH_x F_y$ ($x + y < 3$) radicals as well as appears to be slower in fluorine-rich plasmas. As such, the change in the polymer deposition rate vs. processing conditions may be characterized by the parameter $G2 = \Gamma_{pol}/\Gamma_F$, where Γ_{pol} is the total flux of polymerizing radicals, and Γ_F is the flux of F atoms.

- The destruction of polymer film in oxygen-containing plasmas is provided by both physical (sputtering by ion bombardment) and chemical (etching by oxygen atoms) pathways. Therefore, it is expected that corresponding changes in the polymer film thickness exhibit similar behaviors with $G3 = G2/G1$ and $G4 = G2/\Gamma_O$, where Γ_O is the flux of oxygen atoms.

- In simplest case, the ion-assisted etching mechanism assumes the chemical etching of target surface by F atoms as well as the stimulation of chemical reactions by the ion bombardment. Corresponding mechanisms are normally connected with a) breaking of chemical bonds between surface atoms; and b) the sputtering of low volatile reaction products and/or deposited solid compounds. Accordingly, the parameter $G5 = \Gamma_F/G1$ characterizes the balance between chaotic and directional etching pathways and thus, may be used to trace the change of etching anisotropy.

RESULTS AND DISCUSSION

From plasma diagnostics experiments, it was found that effects of CHF_3/O_2 mixing ratio on electrons- and ions-related plasma parameters (Tab. 1) are quite similar to those found for the O_2/Ar mixing ratio in the $CHF_3 + O_2 + Ar$ plasma [17, 18, 21].

In particular, a monotonic decrease in the electron temperature may surely be associated with increasing electron energy losses in low-threshold excitations processes for O_2 itself and molecular products of plasma chemical reactions, such as FO, CFO, CF_2O , CO and CO_2 (Fig. 1). In the case of O_2 molecules, for instance, such situation is provided by the formation of their metastable states through R1: $O_2 + e \rightarrow O_2(a^1\Delta) +$

e ($\varepsilon_1 = 0.98$ eV) and R2: $O_2 + e \rightarrow O_2(b^1\Sigma) + e$ ($\varepsilon_2 = 1.64$ eV). Obviously, the decreasing fraction of high-energy electrons in EEDF lowers ionization rate coefficients for all type of neutral species and thus, suppresses the formation of electrons and positive ions. In addition, one can also assume that the transition toward O_2 -rich plasmas increases the density of more electronegative species in a gas phase that accelerates the decay of positive ions and electrons through the ion-ion recombination and dissociative attachment, respectively. Therefore, a decrease in J_+ obtained in experiments directly reflects same changes in both n_+ and n_e . The decreasing ion flux $\Gamma_+ \approx J_+/e$ weakens the compensation for the excess negative charge provided by bias power source under the condition of $W_{dc} = \text{const}$. That is why the growth of $-U_{dc}$ takes place. At the same time, the corresponding effect on the ion bombardment energy (262–302 eV for 0–75% O_2) being taken under the square root appears to be smaller compared with the change in Γ_+ . Accordingly, the parameter G1 characterizing the ion bombardment intensity demonstrates the almost two-time fall at 75% O_2 (Table 1).

Table 1

Electrons- and ions-related plasma parameters
Табл. 1. Параметры электронной и ионной компонент плазмы

y(O_2), %	T_e , eV	J_+ , mA/cm ²	$n_+ \approx n_e$, 10^{10} cm ⁻³	$-U_{dc}$, V	$G1, 10^{18}$
0	5.15	1.55	5.09	230	1.12
25	4.72	1.39	4.25	245	0.91
50	4.50	1.24	3.53	255	0.75
75	4.28	1.05	2.84	277	0.61

Note: $G1 = (M_i \varepsilon_i)^{1/2} \Gamma_+$ ($eV^{1/2} cm^{-2} s^{-1}$)

Примечание: $G1 = (M_i \varepsilon_i)^{1/2} \Gamma_+$ ($\varepsilon B^{1/2} cm^{-2} c^{-1}$)

When analyzing kinetics of neutral species, we surely confirmed all features of non-oxygenated CHF_3 -based plasmas known from previous works [16-18, 20]. These are as follows:

1) Among two parallel dissociation mechanisms for CHF_x species, such as R3: $CHF_x + e \rightarrow CHF_{x-1} + F + e$ and R4: $CHF_x + e \rightarrow CF_x + H + e$, the second one is much more effective due to the lower threshold energy. Such situation causes the domination of CF_x over CHF_x radicals, as can be seen from Fig. 1.

2) Gas-phase reactions R5: $CHF_x + F \rightarrow CF_x + HF$ ($k_5 \sim 3.3 \cdot 10^{-11}$ cm³/s for $x = 1$ and 2 while $\sim 1.6 \cdot 10^{-13}$ for $x = 3$), R6: $CHF_x + H \rightarrow CHF_{x-1} + HF$ ($k_6 \sim 3.1 \cdot 10^{-10}$ cm³/s for $x = 1$ and 2) and R7: $CF_x + H \rightarrow CF_{x-1} + HF$ ($k_7 \sim 1.2 \cdot 10^{-11}$ cm³/s for $x = 1$, $\sim 2.2 \cdot 10^{-11}$ cm³/s for $x = 2$ and $\sim 7.9 \cdot 10^{-11}$ cm³/s for $x = 3$) provide the fast conversion of both CF_x and CHF_x species into HF molecules. Accordingly, the latter appears

to be the main gas-phase component (Fig. 1) as well as represent the essential source of F atoms through R8: $\text{HF} + e \rightarrow \text{H} + \text{F} + e$ (by $\sim 45\%$ from total F atom formation rate, as shown in Fig. 2). The almost same F atom production rate is provided by the couple of R9: $\text{CF}_x + e \rightarrow \text{CF}_{x-1} + \text{F} + e$ and R10: $\text{CF}_x + e \rightarrow \text{CF}_{x-1}^+ + \text{F} + 2e$ while contributions of R3, R11: $\text{CF}_x + e \rightarrow \text{CF}_{x-2} + 2\text{F} + e$ and R12: $\text{F}_2 + e \rightarrow 2\text{F} + e$ are below 5%. The last feature is due to either low rate coefficient (for R3 and R11) or the low density of source species (for R12).

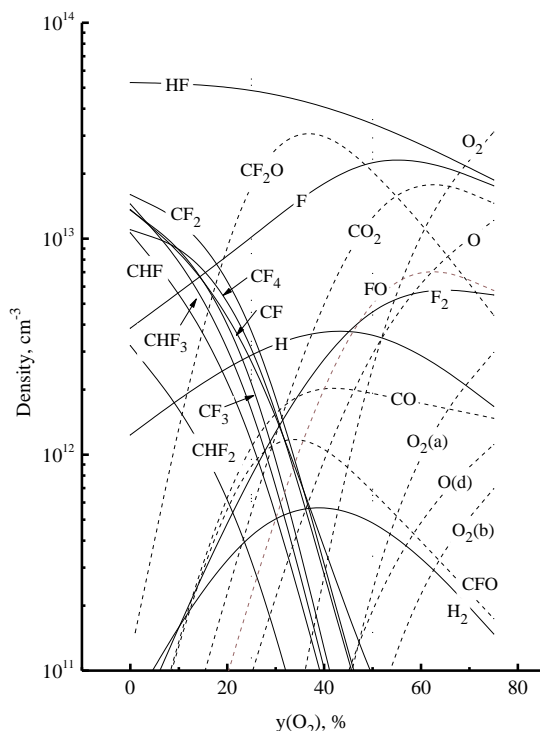


Fig. 1. Steady-state densities of neutral species in $\text{CHF}_3 + \text{O}_2$ plasma. Curves marked as $\text{O}_2(\text{a})$, $\text{O}_2(\text{b})$ and $\text{O}(\text{d})$ correspond to metastable states of $\text{O}_2(\text{a}^1\Delta)$, $\text{O}_2(\text{b}^1\Sigma)$ and $\text{O}(\text{d}^1\text{D})$, respectively. Рис. 1. Стационарные концентрации нейтральных частиц в плазме $\text{CHF}_3 + \text{O}_2$. Метки на кривых $\text{O}_2(\text{a})$, $\text{O}_2(\text{b})$ и $\text{O}(\text{d})$ обозначают метастабильные состояния $\text{O}_2(\text{a}^1\Delta)$, $\text{O}_2(\text{b}^1\Sigma)$ и $\text{O}(\text{d}^1\text{D})$, соответственно

3) The loss of F atoms in R5 dominates over their heterogeneous recombination pathways, such as R13: $\text{F} + \text{CF}_x \rightarrow \text{CF}_{x+1}$ and R14: $\text{F} + \text{F} \rightarrow \text{F}_2$. Accordingly, this provides the condition of $[\text{F}] < [\text{CF}_x]$ (Fig. 1).

An increase in O_2 fraction in a feed gas (in other words, the substitution of CHF_3 for O_2) rapidly suppresses densities of fluorocarbon radicals and increases the density of F atoms (Fig. 1), as have been repeatedly mentioned for $\text{CF}_4 + \text{O}_2$ plasmas [10, 11]. The first effect looks quite understandable and is connected with the conversion of both CF_x and CHF_x into CF_xO species in R14: $\text{CF}_x + \text{O}/\text{O}(\text{d}^1\text{D}) \rightarrow \text{CF}_{x-1}\text{O} + \text{F}$ ($k_{14} \sim 6.1 \cdot 10^{-11} \text{ cm}^3/\text{s}$ for $x = 1$ and $\sim 3.2 \cdot 10^{-11} \text{ cm}^3/\text{s}$ for

$x = 2, 3$), R15: $\text{CHF}_x + \text{O} \rightarrow \text{CF}_x\text{O} + \text{H}$ ($k_{15} \sim 1.1 \cdot 10^{-11} \text{ cm}^3/\text{s}$ for $x = 2$) and R16: $\text{CHF}_x + \text{O} \rightarrow \text{CF}_{x-1}\text{O} + \text{HF}$ ($k_{16} \sim 3.5 \cdot 10^{-11} \text{ cm}^3/\text{s}$ for $x = 1$). Accordingly, increasing densities of CFO and FO molecules result from R14–R16, R17: $\text{CO} + \text{F} \rightarrow \text{CFO}$ ($k_{17} \sim 3.1 \cdot 10^{-11} \text{ cm}^3/\text{s}$) and the heterogeneous process R18: $\text{F} + \text{O} \rightarrow \text{FO}$ while the similar behavior for $[\text{CF}_2\text{O}]$ is due to R19: $\text{CF}_x + \text{CFO} \rightarrow \text{CF}_2\text{O} + \text{CF}_{x-1}$ ($k_{19} \sim 1.1 \cdot 10^{-11} \text{ cm}^3/\text{s}$ for $x = 2$ and $\sim 7.0 \cdot 10^{-13} \text{ cm}^3/\text{s}$ for $x = 1$), R20: $2\text{CFO} \rightarrow \text{CF}_2\text{O} + \text{CO}$ ($k_{20} \sim 1.0 \cdot 10^{-11} \text{ cm}^3/\text{s}$) and R21: $\text{CFO} + \text{F} \rightarrow \text{CF}_2\text{O}$ ($k_{21} \sim 8.0 \cdot 10^{-11} \text{ cm}^3/\text{s}$). Another remarkable fact is the sufficiently increasing density of F_2 molecules (by more than 100 times for 0–75% O_2) that mainly reflects the change of their formation rate in the heterogeneous process R22: $2\text{F} \rightarrow \text{F}_2$.

As for the behavior of F atom density, the situation looks as follows. From published works [10–12], it is known that an increase in $y(\text{O}_2)$ introduces several reaction pathways with CF_x , CF_xO and FO species leading to the formation of F atoms. Under the given set of processing conditions, most effective ones are electron-impact processes R23: $\text{CF}_x\text{O} + e \rightarrow \text{CF}_{x-1}\text{O} + \text{F} + e$ and R24: $\text{FO} + e \rightarrow \text{F} + \text{O} + e$ as well as atom-molecular reactions R14, R25: $\text{FO} + \text{O}/\text{O}(\text{d}^1\text{D}) \rightarrow \text{O}_2 + \text{F}$ ($k_{25} \sim 2.5 \cdot 10^{-11}/5.0 \cdot 10^{-11} \text{ cm}^3/\text{s}$) and R26: $\text{CFO} + \text{O}/\text{O}(\text{d}^1\text{D}) \rightarrow \text{CO}_2 + \text{F}$ ($k_{26} \sim 1.0 \cdot 10^{-10} \text{ cm}^3/\text{s}$). From Fig. 2, it can be seen that the total add-on from R12, R23 and R24 does not overcome the level of R8 and only compensates for decreasing rates of R9 and R10. That is why the overall F atom production rate in electron-impact reactions demonstrates the monotonic decrease toward O_2 -rich plasma following the behavior of R8. The reason is a decrease in both densities of HF molecules (since these are reaction products from CHF_x) and their dissociation frequency (because of sufficient falls in both T_e and n_e , as shown in Table 1).

It can be seen also that the contribution of atom-molecular reactions R14, R25 and R26 begins to be noticeable at $y(\text{O}_2) > 50\%$. Though their cumulative effect finally overlaps the rate of R8, this does not change the decreasing tendency for the total F atom formation rate which appears to be much higher in CHF_3 -rich plasmas. Therefore, one can be sure that an increase in F atom density mentioned in Fig. 1 cannot be related to the same change in their formation kinetics. The analysis of plasma chemistry indicated that the main reason here is the more rapid decrease in the F atom decay frequency in R5 due to decreasing densities of CHF_x species. This conclusion is in agreement with our previous works [16, 17, 20] where the similar mechanism caused the very slow decrease in the F atom density with increasing Ar fraction in the $\text{CHF}_3 + \text{Ar}$ plasma. It is important to note that the above result

is different compared with $\text{CF}_4 + \text{O}_2$ plasma, where the addition of O_2 accelerates the formation as well as increases the density of F atoms exactly through kinetics of R23–R26 [10, 11]. In our opinion, principal differences of $\text{CHF}_3 + \text{O}_2$ gas system are a) the higher dissociation rate coefficient for HF molecules compared with CF_x radicals; and b) the decreasing efficiency for the dissociation of O_2 molecules in R27: $\text{O}_2 + e \rightarrow 2\text{O} + e$ and R28: $\text{O}_2 + e \rightarrow \text{O} + \text{O}(^1\text{D}) + e$ due to a decrease in both T_e and n_e . Accordingly, the last feature limits rates of all process with a participation of atomic oxygen in O_2 -rich plasmas.

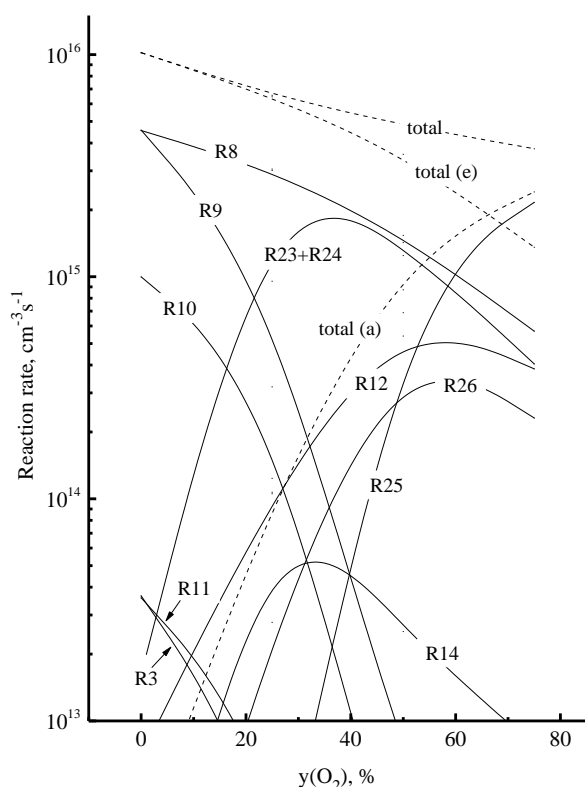


Fig. 2. Fluorine atom formation rates in $\text{CHF}_3 + \text{O}_2$ plasma. Numerical labels on curves correspond to reaction numbers in the text. Curves marked as “total (e)” and “total (a)” illustrate overall effects from electron-impact and atom-molecular reactions, respectively

Рис. 2. Скорости процессов образования атомов фтора в плазме $\text{CHF}_3 + \text{O}_2$. Числовые метки на кривых соответствуют номеру реакции в тексте статьи. Кривые с метками “total (e)” и “total (a)” иллюстрируют суммарные эффекты от реакций под действием электронного удара и атомно-молекулярных процессов, соответственно

Above data on densities of plasma active species allow one to predict some features of heterogeneous process kinetics in the presence of O_2 . As can be seen from Table 2, the total flux of polymerizing radicals demonstrates a monotonic decrease toward O_2 -rich plasma following densities for corresponding species. In a combination with increasing F atom density,

this provides the deeper fall (by more than 3 order of magnitude for 0–75% O_2) in the parameter G2 characterizing the polymer deposition rate. Simultaneously, an increase in both ion bombardment intensity (see the parameter G1 in Table 1) and O atom flux accelerates the destruction of fluorocarbon polymer film by physical and chemical pathways. This reasonably results in the strong influence of $y(\text{O}_2)$ on the polymer film thickness, as can be seen from changes in G3 and G4. Taking into account that the slope for $G4 = f(y(\text{O}_2))$ curve is more drastic compared with that for G3, exactly the oxidative decomposition of polymer film controls its steady-state thickness. The corresponding tendency allows one to suggest that the addition of 25–30% O_2 reduces the plasma polymerizing ability by ~ 100 times. Obviously, this effect is much stronger compared with that for Ar fraction in the $\text{CHF}_3 + \text{Ar}$ plasma under the identical set of processing conditions [16, 17]. Such situation is because the $\text{CHF}_3 + \text{Ar}$ plasma is characterized by the slower fall in G2 (since the density of polymerizing radicals decreases due to the dilution effect only) as well as by the single physical etching pathway for the polymer film.

Table 2
Parameters characterizing heterogeneous process kinetics
Табл. 2. Параметры, характеризующие кинетику гетерогенных процессов

$y(\text{O}_2)$, %	$\Gamma_{\text{pol}}, 10^{16} \text{ cm}^{-2}\text{s}^{-1}$	$G2, 10^{-2}$	$G3, 10^{-20}$	$G4, 10^{-18}$	G5
0	63.5	747.0	667.1	-	0.08
25	17.8	81.1	88.7	294.2	0.24
50	0.17	0.36	0.47	0.03	0.63
75	0.02	0.05	0.08	0.001	0.64

Note: $G2 = \Gamma_{\text{pol}}/\Gamma_{\text{F}}$; $G3 = G2/G1$ ($\text{eV}^{-1/2}\text{cm}^2\text{s}$); $G4 = G2/\Gamma_{\text{O}}$ (cm^2s); and $G5 = \Gamma_{\text{F}}/G1$ ($\text{eV}^{-1/2}$)

Примечание: $G2 = \Gamma_{\text{pol}}/\Gamma_{\text{F}}$; $G3 = G2/G1$ ($\text{эВ}^{-1/2}\text{см}^2\text{с}$); $G4 = G2/\Gamma_{\text{O}}$ ($\text{см}^2\text{с}$); and $G5 = \Gamma_{\text{F}}/G1$ ($\text{эВ}^{-1/2}$)

Finally, we would like to note that the transition toward O_2 -rich plasmas increases the parameter G5 that traces the neutral/charged ratio. Since the latter directly reflects the balance between chaotic and directional etching pathways, one can suggest that an increase in $y(\text{O}_2)$ creates the worse condition for obtaining the anisotropic etching profile. At the same time, this conclusion does not take into account that the oxygen may passivate sidewalls through either the oxidation of surface atoms or the formation of lower volatile oxygen-containing etching products [1–3]. Therefore, for some materials the real effect of oxygen on etching profile features may be weaker or even opposite compared with the change of G5.

CONCLUSIONS

In this work, we investigated how the CHF_3/O_2 mixing ratio in the $\text{CHF}_3 + \text{O}_2$ plasma influences internal plasma parameters (electron temperature, electron density, ion flux and ion bombardment energy), densities of active species and kinetics of fluorine atoms. It was confirmed that, under the given set of processing conditions, the pure CHF_3 plasma is featured by a) the domination of HF molecules among neutral gas-phase components; b) higher densities of CF_x radicals compared with CHF_x species; and c) sufficient influence of $\text{CHF}_x + \text{F} \rightarrow \text{CF}_x + \text{HF}$ reaction family on the F atom decay kinetics. It was shown that an increase in O_2 fraction in a feed gas up to 75% a) lowers the efficiency of electron-impact processes due to a decrease in both electron temperature and density; b) provides the considerable oxidation of CHF_x and CF_x radicals into CF_xO , FO and CO_x compounds; and c) results in increasing F atom density with a maximum value at 50% O_2 . The last phenomenon is not connected with the change in total F atom formation rate, but reflects a drastic decrease of their loss frequency. The model-based analysis of heterogeneous process kinetics indicated that even 25-30% O_2 sufficiently (by more than 100 times) reduce the plasma polymerizing ability.

The work was supported by the Russian Science Foundation grant № 22-29-00216, <https://rscf.ru/project/22-29-00216/>.

Исследование выполнено за счет гранта Российского научного фонда № 22-29-00216, <https://rscf.ru/project/22-29-00216/>.

Авторы заявляют об отсутствии конфликта интересов, требующего раскрытия в данной статье.

The authors declare the absence a conflict of interest warranting disclosure in this article.

REFERENCES

ЛИТЕРАТУРА

1. **Nojiri K.** Dry etching technology for semiconductors. Tokyo: Springer Internat. Publ. 2015. 116 p. DOI: 10.1007/978-3-319-10295-5.
2. Advanced plasma processing technology. New York: John Wiley & Sons Inc. 2008. 479 p.
3. **Wolf S., Tauber R.N.** Silicon Processing for the VLSI Era. Volume 1. Process Technology. New York: Lattice Press. 2000. 416 p.
4. **Lieberman M.A., Lichtenberg A.J.** Principles of plasma discharges and materials processing. New York: John Wiley & Sons Inc. 2005. 757 p. DOI: 10.1002/0471724254.
5. **Donnelly V.M., Kornblit A.** Plasma etching: Yesterday, today, and tomorrow. *J. Vac. Sci. Technol.* 2013. V. 31. P. 050825-48. DOI: 10.1116/1.4819316.
6. **Standaert T.E.F.M., Hedlund C., Joseph E.A., Oehrlein G.S., Dalton T.J.** Role of fluorocarbon film formation in the etching of silicon, silicon dioxide, silicon nitride, and amorphous hydrogenated silicon carbide. *J. Vac. Sci. Technol. A.* 2004. V. 22. P. 53-60. DOI: 10.1116/1.1626642.
7. **Schaepkens M., Standaert T.E.F.M., Rueger N.R., Sebel P.G.M., Oehrlein G.S., Cook J.M.** Study of the SiO_2 -to- Si_3N_4 etch selectivity mechanism in inductively coupled fluorocarbon plasmas and a comparison with the SiO_2 -to-Si mechanism. *J. Vac. Sci. Technol. A.* 1999. V. 17. P. 26-37. DOI: 10.1116/1.582108.
8. **Kastenmeier B.E.E., Matsuo P.J., Oehrlein G.S.** Highly selective etching of silicon nitride over silicon and silicon dioxide. *J. Vac. Sci. Technol. A.* 1999. V. 17. P. 3179-3184. DOI: 10.1116/1.58209.
9. **Marra D.C., Aydil E.S.** Effect of H_2 addition on surface reactions during CF_4/H_2 plasma etching of silicon and silicon dioxide films. *J. Vac. Sci. Technol. A.* 1997. V. 15. P. 2508-2516. DOI: 10.1116/1.580762.
10. **Kimura T., Noto M.** Experimental study and global model of inductively coupled CF_4/O_2 discharges. *J. Appl. Phys.* 2006. V. 100. P. 063303 (1-9). DOI: 10.1063/1.2345461.
11. **Efremov A., Lee J., Kim J.** On the Control of Plasma Parameters and Active Species Kinetics in $\text{CF}_4 + \text{O}_2 + \text{Ar}$ Gas Mixture by CF_4/O_2 and O_2/Ar Mixing Ratios. *Plasma Chem. Plasma Proc.* 2017. V. 37. P. 1445-1462. DOI: 10.1007/s11090-017-9820-z.
12. **Chun I., Efremov A., Yeom G. Y., Kwon K.-H.** A comparative study of $\text{CF}_4/\text{O}_2/\text{Ar}$ and $\text{C}_4\text{F}_8/\text{O}_2/\text{Ar}$ plasmas for dry etching applications. *Thin Solid Films.* 2015. V. 579. P. 136-143. DOI: 10.1016/j.tsf.2015.02.060.
13. **Efremov A.M., Betelin V.B., Mednikov K.A., Kwon K.-H.** Gas-phase parameters and reactive-ion etching regimes for Si and SiO_2 in binary Ar + $\text{CF}_4/\text{C}_4\text{F}_8$ mixtures. *ChemChemTech [Izv. Vyssh. Uchebn. Zaved. Khim. Khim. Tekhnol.]*. 2021. V. 64. N 6. P. 25-34.
Ефремов А.М., Бетелин В.Б., Медников К.А., Кwon К.-Н. Параметры газовой фазы и режимы реактивно-ионного травления Si и SiO_2 в бинарных смесях Ar + $\text{CF}_4/\text{C}_4\text{F}_8$. *Изв. вузов. Химия и хим. технология.* 2021. Т. 64. Вып. 6. С. 25-34 DOI: 10.6060/ivkkt.20216406.6377.
14. **Kokkoris G., Goodyear A., Cooke M., Gogolides E.** A global model for C_4F_8 plasmas coupling gas phase and wall surface reaction kinetics. *J. Phys. D. Appl. Phys.* 2008. V. 41. P. 195211 (1-12). DOI: 10.1088/0022-3727/41/19/195211.
15. **Lee B. J., Efremov A., Nam Y., Kwon K.-H.** Plasma Parameters and Silicon Etching Kinetics in $\text{C}_4\text{F}_8 + \text{O}_2 + \text{Ar}$ Gas Mixture: Effect of Component Mixing Ratios. *Plasma Chem. Plasma Proc.* 2020. V. 40. P. 1365-1380. DOI: 10.1007/s11090-020-10097-9.
16. **Efremov A., Murin D., Kwon K.-H.** Concerning the Effect of Type of Fluorocarbon Gas on the Output Characteristics of the Reactive-Ion Etching Process. *Russ. Microelectronics.* 2020. V. 49. N 3. P. 157-165. DOI: 10.1134/S1063739720020031.
17. **Lim N., Efremov A., Kwon K.-H.** A comparison of CF_4 , CHF_3 and $\text{C}_4\text{F}_8 + \text{Ar}/\text{O}_2$ Inductively Coupled Plasmas for Dry Etching Applications. *Plasma Chem. Plasma Proc.* 2021. V. 41. P. 1671-1689. DOI: 10.1007/s11090-021-10198-z.

18. **Efremov A., Lee B.J., Kwon K.-H.** On Relationships Between Gas-Phase Chemistry and Reactive-Ion Etching Kinetics for Silicon-Based Thin Films (SiC, SiO₂ and Si_xN_y) in Multi-Component Fluorocarbon Gas Mixtures. *Materials*. 2021. V. 14. P. 1432(1-27). DOI: 10.3390/ma14061432.
19. **Shun'ko E.V.** Langmuir probe in theory and practice. Boca Raton: Universal Publ. 2008. 245 p.
20. **Efremov A. M., Murin D. B., Kwon K. H.** Parameters of plasma and kinetics of active particles in CF₄(CHF₃) + Ar mixtures of a variable initial composition. *Russ. Microelectronics*. 2018. V. 47(6). P. 371-380. DOI: 10.1134/S1063739718060033.
21. **Efremov A.M., Murin D.B., Kwon K.-H.** Plasma Parameters and Kinetics of Active Particles in the Mixture CHF₃ + O₂ + Ar. *Russ. Microelectronics*. 2020. V. 49(4). P. 233-243. DOI: 10.1134/S1063739720030038.
22. **Hsu C.C., Nierode M.A., Coburn J.W., Graves D.B.** Comparison of model and experiment for Ar, Ar/O₂ and Ar/O₂/Cl₂ inductively coupled plasmas. *J. Phys. D. Appl. Phys.* 2006. V. 39. P. 3272-3284. DOI: 10.1088/0022-3727/39/15/009.
23. **Ho P., Johannes J.E., Buss R.J.** Modeling the plasma chemistry of C₂F₆ and CHF₃ etching of silicon dioxide, with comparisons to etch rate and diagnostic data. *J. Vac. Sci. Technol. B*. 2001. V. 19. P. 2344-2367. DOI: 10.1116/1.1387048.
24. **Gray D.C., Tepermeister I., Sawin H.H.** Phenomenological modeling of ion-enhanced surface kinetics in fluorine-based plasma-etching. *J. Vac. Sci. Technol. B*. 1993. V. 11. P. 1243-1257. DOI: 10.1116/1.586925.
25. **Chapman B.** Glow Discharge Processes: Sputtering and Plasma Etching. New York: John Wiley & Sons Inc. 1980. 432 p.

Поступила в редакцию 16.05.2022

Принята к опубликованию 29.09.2022

Received 16.05.2022

Accepted 29.09.2022